

NASA Technical Memorandum 105984
AIAA-93-0249

Optimization of Circular Orifice Jets Mixing Into a Heated Cross Flow in a Cylindrical Duct

J.T. Kroll, W.A. Sowa, and G.S. Samuelson
University of California
Irvine, California

and

J.D. Holdeman
Lewis Research Center
Cleveland, Ohio

Corrected Copy

Prepared for the
31st Aerospace Sciences Meeting
sponsored by the American Institute of Aeronautics and Astronautics
Reno, Nevada, January 11-14, 1993



OPTIMIZATION OF CIRCULAR ORIFICE JETS MIXING INTO A HEATED CROSSFLOW IN A CYLINDRICAL DUCT

J.T. Kroll, * W.A. Sowa,† G.S. Samuelsen‡
UCI Combustion Laboratory
University of California
Irvine, CA 92717-3550

J.D. Holdeman§
NASA Lewis Research Center
Cleveland, Ohio 44135

ABSTRACT

To examine the mixing characteristics of circular jets in an axi-symmetric can geometry, temperature measurements were obtained downstream of a row of cold jets injected into a heated cross stream. The objective of the research was to obtain uniform mixing within one duct radius downstream of the leading edge of the jet orifices. An area weighted standard deviation of the mixture fraction was used to help quantify the degree of mixedness at a given plane. Non-reacting experiments were conducted to determine the influence of the number of jets on the mixedness in a cylindrical configuration. Results show that the number of orifices significantly impacts the mixing characteristics of jets injected from round hole orifices in a can geometry. Optimum mixing occurs when the mean jet trajectory aligns with the radius which divides the cross sectional area of the can into two equal parts at one mixer radius downstream of the leading edge of the orifice. The optimum number of holes at momentum-flux ratios of 25 and 52 is 10 and 15 respectively.

LIST OF SYMBOLS

f	mixture fraction
J	jet to mainstream momentum-flux ratio
X6	prefix for six orifice module
X8	prefix for eight orifice module
X10	prefix for ten orifice module
X12	prefix for twelve orifice module
X15	prefix for fifteen orifice module
X18	prefix for eighteen orifice module

-
- * Graduate Student Researcher
† Associate Director UCICL, Member AIAA
‡ Professor, Corresponding Author, Associate Fellow AIAA
§ Senior Research Engineer, Associate Fellow AIAA

MR	jet to mainstream mass-flow ratio
DR	jet to mainstream density ratio
z	axial distance, zero at orifice leading edge
R	mixer radius, 1.5 inches
d	jet orifice diameter
z/R	normalized axial distance downstream of the leading edge of the orifice
z/d	normalized axial distance downstream of the leading edge of the orifice

INTRODUCTION

Jets-in-crossflow are an integral constituent flow in a number of areas important in combustion and energy science and technology.

In a gas turbine combustor for example, mixing of relatively cold air jets can significantly affect both combustor efficiency and emissions. Jets in a subsonic crossflow are also encountered in other airborne and terrestrial combustion applications, such as in premixing of fuel and air. In addition, mixing of transverse jets is important in applications such as the discharge of effluent in water, and in transition from hover to cruise for STOVL aircraft.

One characteristic of combustor applications is that these are confined mixing problems. The result is that the equilibrium temperature and composition of the exiting flow will differ significantly from that of the entering mainstream flow, even if the flow is not reacting.

A scheme proposed for advanced aeropropulsion engine combustors is the Rich Burn/Quick Mix/Lean Burn (RQL) combustor¹. This concept involves beginning the combustion process in a fuel rich zone, and completing it in a fuel lean zone to minimize regions of near stoichiometric fuel air ratio where NO_x production would be expected to be greatest. One key to a successful RQL combustor is an efficient mixing section that carries out the dilution process rapidly and uniformly.

BACKGROUND

Hatch et al.² studied the mixing characteristics of both circular and slanted slot jet orifices in a cylindrical duct, where the number of orifices for each mixer was held constant at eight. Mixing performance was observed to be strongly dependent on momentum-flux ratio as well as orifice design. Moreover, the need to consider configurations with more than eight orifices was evident. At a jet to mainstream momentum-flux ratio of 25, it appeared that the eight orifice round hole module had near optimal penetration, whereas flow from slanted slot modules showed severe under penetration. While a comparison between unoptimized orifice geometries provides a basic understanding of the different mixing mechanisms at work, it is necessary to compare optimized geometries in order to select one orifice design over the other.

The majority of the previous research on jets-in-a-confined-crossflow has been performed in rectangular geometries. The influence of orifice geometry and spacing, jet-to-mainstream momentum-flux ratio (J), and density ratio (DR) has been summarized for single and double sided injection by Holdeman³. More recent studies of jets in a confined crossflow in a rectangular duct have been reported by Smith⁴, Liscinsky et al.⁵, and Bain et al.⁶

As a result of these studies, momentum-flux ratio and orifice geometry and spacing have been identified as the dominant parameters influencing the mixing. These observations are supported by the findings of Hatch et al.² who observed that, even though eight circular orifices at a momentum-flux ratio (J) of 25 provide optimum mixing, eight

circular jets at $J=80$ over-penetrated and impinge upon one another at the module's center line resulting in deteriorated mixing. Further support to the theory of an optimum number of orifices at a given momentum-flux ratio is provided by Liscinsky et al.⁵

Analyses and experiments of jet mixing in a can have been reported by Bruce et al.⁷ Among the results therein, is the hypothesis that the effective orifice spacing is that at half the radius of the can. A computational study reported by Holdeman et al.⁸ suggested that results for a rectangular duct and a can were similar if the orifice spacing for the latter were specified at the radius that divides the can into equal areas. Recent experimental and computational studies in a cylindrical geometry are reported in Talpallikar et al.⁹, Smith et al.¹⁰, Vranos et al.¹¹, and Oechsle et al.¹²

A computational study of mixing was conducted by Oechsle et al.¹² for square, elongated slot, and equilateral triangle orifice configurations. The study concluded that mixing can be detrimentally effected by either under or over penetrating jets. Under penetrating jets allowed an undiluted core of main flow to pass through the mixing section. Similarly, over penetrating jets provide the opportunity for pure main flow to escape along the walls of the mixing section.

EXPERIMENT

A series of experiments was conducted to determine the influence of the number of circular orifices on mixing of jets in a can geometry. The parametric experiments were investigated at J values of 25 and 52, while maintaining a jet to mainstream mass-flow ratio of 2.2. An area discharge coefficient of 0.80 was assumed in designing the orifices.

Table 1: Mixing module configurations considered.

Momentum-flux Ratio	Number of Orifices	Momentum-flux Ratio	Number of Orifices
25	6	52	6
25	8	52	8
25	10	52	10
25	12	52	12
		52	15
		52	18

Table 2: Operating Conditions

T_{main} (°F)	T_{jet} (°F)	P (psia)	V_{main} (fps)	M_{main} (pps)	Mass-flow ratio	Density Ratio
212	74	14.7	34.5	0.10	2.2	1.26

The modules tested in this study were fabricated from 3-inch inside diameter, 0.125-inch thick acrylic tubing. Each orifice configuration was manufactured with equally spaced orifices around the circumference of the module. Table 1 summarizes the experiments that were conducted.

Mixing was quantified by measuring and recording the fluid temperature at several discrete points. The mainstream flow entering the module was heated to 212°F, the upper limit of the acrylic tubing used. The jets were introduced at room temperature.

The operating conditions are presented in Table 2. Reference velocity, defined as the velocity at the inlet to the mixing section and calculated based on the mainstream temperature and pressure, was 34.5 fps. The actual discharge coefficient and momentum-flux ratio for each case were determined by measuring the jet pressure drop across the mixing module. As a note, all ratios (momentum-flux, mass, and density) are expressed as jet flow divided by main flow.

A 12-inch long, 0.125-inch diameter type K thermocouple was used to measure the temperatures. The thermocouple was held in a fixed position while the test assembly was traversed in the x, y, and z directions. The temperature measurements were

made at five to eight planes per module across a two orifice sector. The data point sector mapping was customized for each module to ensure that adequate resolution was achieved to capture the strong thermal gradients near the orifice region. Figure 1 shows typical measurement points and axial planes. The planes examined in this study were located between 0.125 inches upstream of the leading edge of the orifices, and one module radius downstream of the leading edge of the orifices.

The experimental facility is the same one that Hatch et al.² used for conducting influence of orifice geometry and flow variations mixing experiments. A complete description of the facility can be found in Reference 2.

The axial location of the trailing edge of the orifice, and the circumferential orifice blockage are presented in Table 3. The former is expressed as the ratio of the diameter of the orifice to the radius of the mixing module, and the latter is defined as the ratio of the circumferential projection of the orifice to the spacing between orifice centers.

A schematic of each mixing configuration for both the J=52 and the J=25 experiments is illustrated in Figures 2 and 3 respectively. The orifice diameters are expressed in terms of the ratio d/R.

Table 3. Axial Location of Orifice Trailing Edge, and Orifice Blockage

Momentum Flux Ratio	Number of Orifices	d/R	Blockage
J=25	6	0.58	0.56
J=25	8	0.50	0.64
J=25	10	0.45	0.72
J=25	12	0.41	0.78
J=52	6	0.48	0.46
J=52	8	0.42	0.53
J=52	10	0.37	0.60
J=52	12	0.34	0.65
J=52	15	0.30	0.73
J=52	18	0.28	0.80

ANALYSIS

To compare the mixing characteristics of different modules, the temperature measurements were normalized by defining the mixture fraction, f , at each point in the plane:

$$f = \frac{T_{\text{measured}} - T_{\text{jet}}}{T_{\text{main}} - T_{\text{jet}}}$$

A value of $f=1.0$ corresponds to the mainstream temperature, while $f=0$ indicates the presence of pure jet flow. Complete mixing occurs when f approaches the equilibrium value determined by the mass-flow ratio and temperatures of the jet and mainstreams. Under the conditions at which these experiments were conducted, as shown in Table 2, $f_{\text{equil}}=0.3125$, which is the mixture fraction calculated when $T_{\text{measured}}=T_{\text{equil}}$. Note that $f = 1 - \theta$, where θ has been used previously (e.g. Reference 3), and that f_{equil} is equal to the ratio of the approach flow to the total flow.

To quantify the mixing effectiveness of each module configuration, an area-weighted standard deviation

parameter ("STD") was defined at each measurement and interpolated data plane.

$$STD = \sqrt{\frac{1}{A} \sum a_i (f_i - \bar{f})^2}$$

\bar{f} is the average planar mixture fraction, a_i is the nodal area at which f_i is calculated, and $A = \sum a_i$. It should be noted that at planes downstream of the trailing edge of the orifice, \bar{f} equals the equilibrium mixture fraction. Complete mixing is achieved when the STD across a given plane reaches zero.

The STD differs from the Mixture Uniformity defined by Hatch et al.² in that STD is based on the mean mixture fraction for the plane at which the parameter is applied, whereas the Mixture Uniformity is based on the equilibrium mixture fraction after all the jet mass is added. The STD has been applied here to examine the mixture fraction deviation in the orifice region where mass addition is taking place. Note that the STD is equivalent to the Mixture Uniformity in the region downstream of the orifices, where the mean mixture fraction becomes equivalent to the equilibrium mixture fraction.

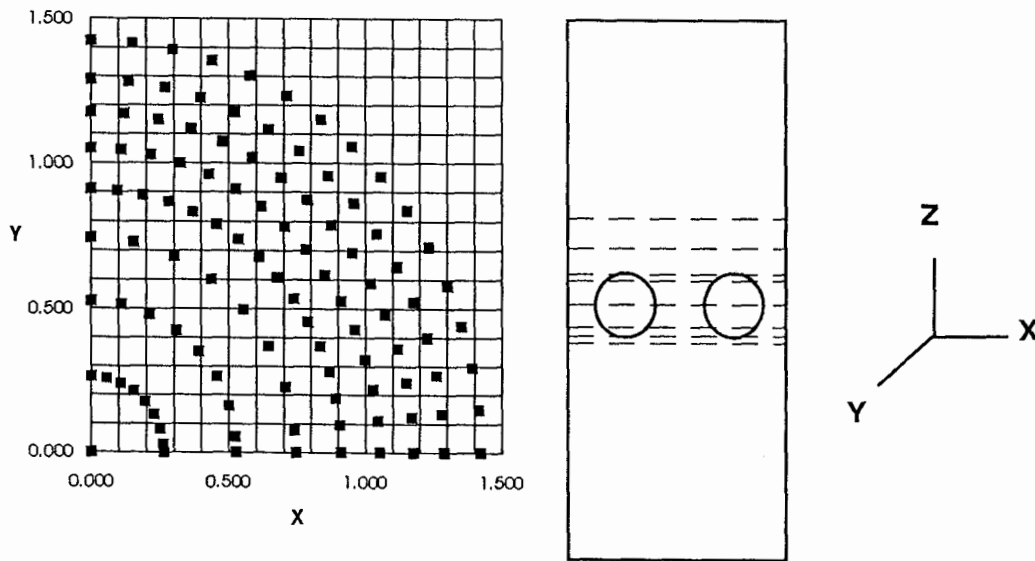


Figure 1. Measurement Points and Planes

RESULTS AND DISCUSSION

This study has focused on two momentum-flux ratios (J): J=25 and J=52. Inasmuch as the trends are similar in both cases, the results for momentum-flux ratios of 52 are discussed first followed by a summary of the results for momentum-flux ratios of 25. In those cases where there are significant differences in the results between the two momentum-flux ratios, these differences are clearly delineated.

To facilitate the analysis of the mixing performance of the different round hole orifice modules, a division was made between in-orifice mixing and downstream mixing. The in-orifice mixing is where mass addition is occurring. Due to the mass addition, the strongest gradients for non-reacting systems exist in that region. The downstream mixing is characterized by the relaxation of the strong gradients that exist in the orifice through convective and diffusive mixing. In the downstream mixing region the mean orifice jet trajectories become significant in dictating the overall uniformity of mixing that is achieved.

Mixing in the Orifice

Mass Addition Characteristics of J52 Configurations

The calculated percentages of jet mass added for two axial planes within the orifice as a function of the number of orifices for an overall momentum-flux ratio of 52 are shown in Figure 4. (The J=25 equivalent is shown in Figure 5.) These calculations are based on the average mixture fraction across the plane of interest, and are arrived at with the following equation.

$$\text{mass addition} = 100 * \frac{f_{eq}}{\bar{f}_i} * \frac{1 - \bar{f}_i}{1 - f_{eq}}$$

The accuracy of this calculation was determined to be within 4%.

The light gray bars show the percent jet mass existing at the axial plane at the leading edge of the orifice. The darker bars show the jet mass existing at the axial plane midway through the orifice. At the leading edge plane of the orifices, none of the modules at a momentum-flux ratio of 52 had less than 25% of the total jet flow mass addition completed. By the orifice mid-plane, most of the modules had completed the mass addition process. The explanation for this mass addition characteristic

is apparently tied to jet material being transported upstream of the orifices. Two mechanisms are likely responsible; namely, jet impingement at the module's center line resulting in the redirection of jet flow in both the up stream and down stream directions, and re-circulation zones around the circumference of the orifices.

It is interesting to note that the lowest value of jet stream mass addition at the leading edge of the orifice is displayed by the 15 orifice module. In going from the 6 orifice module to the 15 orifice module, the J=52 modules illustrate a decline in jet mass added by the leading edge plane of the orifice. This trend was anticipated due to the decrease in jet penetration and associated impingement at the modules center line as a function of increasing orifice number. The surprise here is that the 18 orifice module has a greater amount of mass added at the orifice leading edge plane than that of the 15 orifice module. This increase is attributed to a greater degree of re-circulation around the circumference of the orifices.

Another perspective on the jet mass addition process is shown in Figure 6. In this figure, percent jet mass added is plotted relative to the normalized orifice diameter (z/d) for each J=52 module. The normalized orifice diameter is defined as the axial distance downstream of the leading edge of the orifice (z), divided by the orifice diameter (d). (The number of orifices for each module is shown in the legend following the letter X.) The normalized distances of 0 and 1 correspond to the leading and trailing edges of each orifice respectively. Like Figure 4, this figure also shows that the lowest rate of mass addition occurs for the 15 hole module, and that the entire mass addition process is nearly complete midway through the orifice.

Mass Addition Characteristics of J25 Configurations

Figure 7 shows the mass addition process for the J=25 modules. Two differences stand out between the cases shown in Figures 6 and 7. First, the amount of jet mass transported upstream of the orifice is less for the lower momentum-flux ratio cases. Second, the lowest rate of mass addition occurs now for a ten hole module. Many trends are also similar. When the jets are over penetrating (as the X6J25 module was observed to be) or under penetrating (as the X12J25 module was observed to be) the rate of mass addition increases.

Note that a true mass conservation could not be calculated at each plane as the velocity field was not

measured. Also, jet exit measurements may be useful as the jet exit boundary conditions are otherwise unknown.

Mixture Uniformity

In the region bounded by the leading and trailing edges of the orifice, two primary mixing mechanisms are at work: (1) direct jet interaction with the main flow, and (2) small scale mixing around the circumference of the orifices due to recirculation zones.

Figures 8 and 9 show the standard deviation parameter (STD) as a function of the normalized orifice diameter. These figures suggest that, regardless of the number of orifices, the standard deviation in mixture fraction peaks in magnitude near the mid plane of the orifices, then decreases thereafter. Recall that for the $J=52$ momentum-flux modules, the large majority of jet mass has been added by the orifice mid plane. At the completion of the mass addition process, each module experiences the convective and diffusion mixing processes that relax the gradients created from mass addition. This characteristic is the same for the $J=25$ momentum-flux ratio cases considered.

For both the $J=25$ and $J=52$ cases, the modules that added mass most slowly displayed the most uniformity at the trailing edge axial plane of the orifice.

Mixing Downstream of the Orifice

Influence of Jet Trajectories

It is necessary to examine the downstream mixing to better understand the mixing processes occurring in each module. In particular, the mean jet trajectory

provides much insight into what is happening in the overall mixing process. Figures 10 and 11 depict radial-axial slices, which have been selected near the center of the orifices, of mixture fraction values for $J=52$ and $J=25$ respectively. The mainstream is flowing from left to right, and the jet is discharging downward from the top of the figure toward the centerline of the module at the bottom of the figure. These figures were created by linearly interpolating between a maximum of eight measured data planes. They are, therefore, useful for trend analysis, but should not be considered absolutely quantitative at all points.

The intent of Figures 10 and 11 is to obtain an intuitive feel for the jet trajectory. As such, they can be used to make qualitative comparisons between modules, but should not be used to make quantitative comparisons between modules. Additionally, note that these are specific radial-axial planes near the orifice center-line, and not an average over several planes.

In Figures 10 and 11, radial distance is measured from the module centerline ($r/R=0$) to the module wall ($r/R=1.0$). The axial distance is measured from the leading edge of the orifice ($z/R=0$) to one duct radius downstream ($z/R=1.0$). The mean jet trajectory can be traced by following the lowest values of mixture fraction downstream from their point of origin at the module wall. From these figures, it can be seen qualitatively that the mean jet trajectory is strongly correlated with the number of orifices.

Figure 12 illustrates different characteristics of the jet trajectory that can be estimated semi-quantitatively from Figure 10 and 11. In total, three characteristics have been examined: linear

Table 4: Semi-Quantitative Jet Trajectory Characteristics For $J=52$ Round Hole Modules

Number of Orifices	Linear Penetration Depth (%)	% Mean Jet Penetration Depth @ $z/R=1$	Center Line Impingement
6	33	100	intersects
8	25	76	will intersect upstream of $z/R=1$
10	12	72	likely will intersect upstream of $z/R=1$
12	8	62	likely will not intersect upstream of $z/R=1$
15	5	44	will not intersect
18	3	24	definitely will not intersect

penetration depth, the mean jet penetration depth at $z/R=1$, and the likelihood that the mean jet trajectory will penetrate to the module's centerline. Linear penetration depth characterizes the normalized distance from the module wall that the jet travels before deflection is apparent in the axial direction. The jet penetration depth was estimated from experimental data for the plane at one duct radius downstream of the leading edge of the orifice. It is a distance normalized by the module radius which tracks how far from the module wall the lowest mixture fraction value is found. The likelihood that the mean jet trajectory will intersect with the module centerline can be estimated based on observations of the rate of change of the mean jet trajectory.

Table 4 summarizes the three characteristics discussed above for the $J=52$ cases shown in Figure 10. It should be noted that of the six cases considered at $J=52$, only three had mean jet trajectories that likely intersected with the module centerline. It is also noteworthy that the 15 hole module which showed the most uniform mixing at the trailing edge of the orifice had a jet penetration distance of only 44 percent of the module radius measured from the module wall. The $J=25$ jet penetration results are similar to those discussed above, albeit the change from penetration that intersects the centerline to that which stays near the wall occurs in the range from six orifices per module to twelve orifices per module. The most uniformly mixed module at $J=25$ (the ten hole module) has a jet penetration distance normalized by the module radius of 35 percent as measured from the module wall.

Mixing at One Duct Radius Downstream

From Figures 10 and 11, coupled with Table 4, one can obtain an intuitive feeling of the mixing process that is taking place in the module. However, more information is needed to select an optimum mixer. Figures 13 and 14 address this issue.

As noted previously, a perfectly mixed plane of fluid would have a mixture fraction STD of zero. Figure 13 shows the mixture fraction STD as a function of distance normalized from the leading edge of the orifice ($z/R = 0.0$) to one duct radius downstream ($z/R = 1.0$) for the $J=52$ modules. As was seen at the trailing edge of the orifice, the mixture uniformity as characterized by the STD values decrease as the number of orifices increases until the optimum number is reached and thereafter the value increases. As is suggested in Figure 10, the 15 orifice module yields the most uniform mixing. Figure 14 is the

$J=25$ analogy to Figure 13. The trends are the same for both the $J=25$ and $J=52$ cases.

Figure 15 depicts the mean jet penetration depth at one mixer radius downstream of the leading edge of the orifices as a function of orifice number for the $J=52$ modules. Here we observe that the best mixers, namely the 12, 15, and 18 orifice modules, all display a penetration depth between 20% and 60% of the distance between the wall and the module's center line. Not coincidentally, the radius that divides the module's cross-section into an equal area circle and annulus, occurs at 30% of the distance from the wall (a "half area radius"). This suggests that the optimum mixer would likely be the one where the mean jet trajectory ended up on the "half area radius". At this penetration depth, the jet fluid would be exposed to equal amounts of mainstream material on either side of the jet.

These results agree with the relation proposed by Holdeman³ for optimal mixing in a can configuration, where the number of orifices (n) is

$$n = \pi\sqrt{2J} / C$$

With $C=2.5$, as was reported to result in optimum one-side mixing in a rectangular geometry, thirteen orifices is predicted for $J=52$, and nine orifices is predicted for $J=25$.

SUMMARY AND CONCLUSION

Non-reacting mixing experiments were conducted to delineate the correlation between mixing performance and orifice number for round hole orifices. These experiments were conducted at momentum-flux ratios of 25 and 52. Mixing both inside and downstream of the orifice was examined by characterizing the mass addition performance, planar uniformity about a mean mixture fraction value, and jet penetration.

It was calculated that nearly 100% of the jet stream mass was added by the orifice mid-plane for the $J=52$ modules while more than 45% of the jet stream mass was added by the orifice mid-plane for the $J=25$ modules. The slowest mass addition rate was observed for those modules that were best mixed at one duct radius downstream. The mass addition rate was strongly correlated to the extent to which the jet material was convected upstream of the orifice leading edge. The transport of jet mass material upstream of the orifice leading edge is likely influenced by two mechanisms: jet-jet interaction on the module centerline (which was significant for over penetrating modules with fewer orifices), and near

wall recirculation of the jet mass as it enters the larger duct.

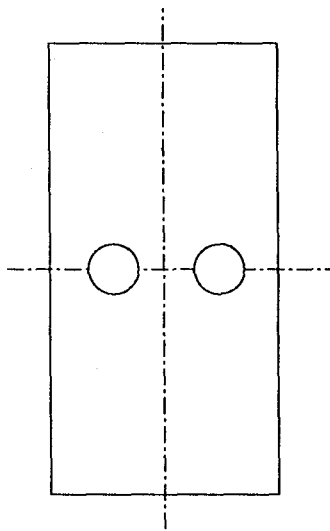
To yield the most uniform mixing at one duct radius downstream of the leading edge of the orifice, the analysis of the down stream mixing revealed that the mean jet trajectory needs to end up close to the module's half area radius. This observation was true for both $J=25$ and the $J=52$ momentum-flux ratio modules considered. The $J=25$ momentum-flux ratio modules required fewer holes than the $J=52$ momentum-flux ratio modules to have the jet trajectory be optimum for most uniform mixing.

ACKNOWLEDGMENTS

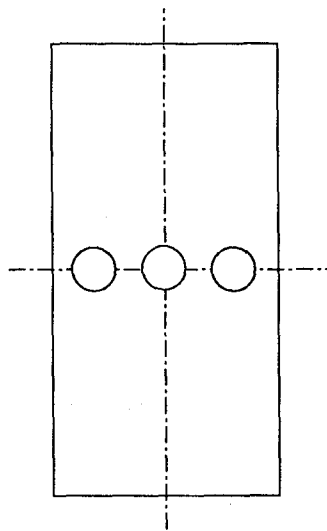
This work is an integral component of a program supported by the NASA-Lewis Research Center (Grant NAG3-1110).

REFERENCES

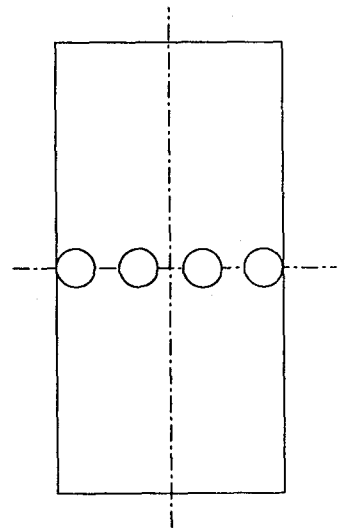
1. Shaw, R.J., "Engine Technology Challenges for a 21st Century High Speed Civil Transport," AIAA Tenth International Symposium on Air Breathing Engines, September 1-6, 1991 (also NASA TM 104363).
2. Hatch, M.S., Sowa, W.A., Samuelsen, G.S., and Holdeman, J. D., "Jet Mixing Into a Heated Cross Flow in a Cylindrical Duct: Influence of Geometry and Flow Variations," AIAA-92-0773, 1992. (also NASA TM 105390).
3. Holdeman, J. D., "Mixing of Multiple Jets with a Confined Subsonic Crossflow," AIAA-91-2458, 1991. (also NASA TM 104412).
4. Smith, C.E., "Mixing Characteristics of Dilution Jets in Small Gas Turbine Combustors," AIAA-90-2728, 1990.
5. Liscinsky, D.S., True, B., Vranos, A., and Holdeman, J. D., "Experimental Study of Cross-Stream Mixing in a Rectangular Duct," AIAA-92-3090, 1992. (also NASA TM 105694).
6. Bain, D.B., Smith, C.E., and Holdeman, J.D. "CFD Mixing Analysis of Jets Injected from Straight and Slanted Slots into Confined Crossflow in Rectangular Ducts," AIAA 92-3087, 1992. (also NASA TM 105699).
7. Bruce, T.W., Mongia, H.C., and Reynolds, R.S. "Combustor Design Criteria Validation," AiResearch Manufacturing Co., Phoenix, AZ, AiResearch 75-211682(38)-1, March 1979. (USARTL-TR-78-55A).
8. Holdeman, J.D., Srinivasan, R., Reynolds, R., and White, C.D. "Studies of the Effects of Curvature on Dilution Jet Mixing," J. of Propulsion and Power, vol. 7, no. 4, Jul-Aug 1991. (see also AIAA-87-1953 (NASA TM 89878) & AIAA-88-3180 (NASA TM 100896)).
9. Talpallikar, M.V., Smith, C.E., Lai, M.C., and Holdeman, J.D. "CFD Analysis of Jet Mixing in Low NO_x Flametube Combustors," AIAA 91-217, 1991. (also NASA TM 104466).
10. Smith, C.E., Talpallikar, M.V., and Holdeman, J.D. "Jet Mixing in Reduced Areas for Lower Combustor Emissions in Gas Turbine Combustors," AIAA 91-2460, 1991. (also NASA TM 104411).
11. Vranos, A., Liscinsky, D., True, B., and Holdeman, J.D. "Experimental Study of Cross-Stream Mixing in a RQL Combustor Quench Section Model," AIAA 91-2459, 1991. (also NASA TM 105180).
12. Oechsle, V.L., Mongia, H.C., and Holdeman, J. D., "A Parametric Numerical Study of Mixing in a Cylindrical Duct," AIAA-92-3088, 1992. (also NASA TM 105695).



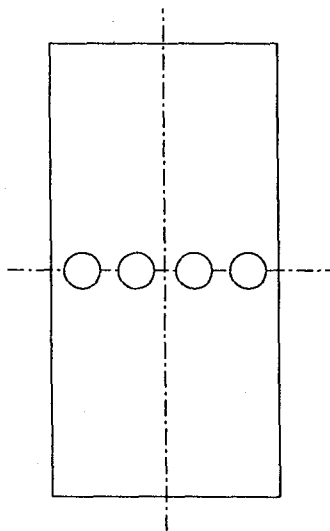
Six Orifice Mixer
 $d/R = 0.48$



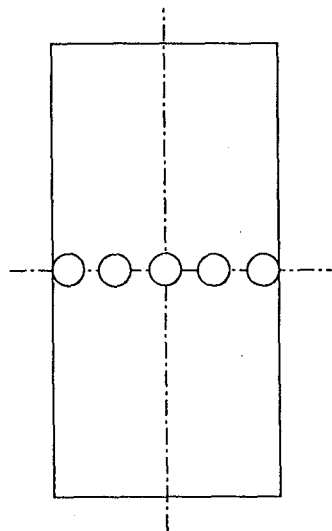
Eight Orifice Mixer
 $d/R = 0.42$



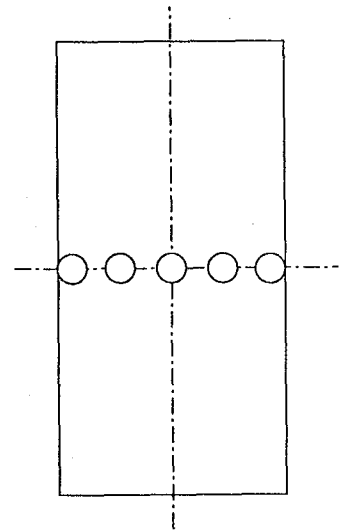
Ten Orifice Mixer
 $d/R = 0.37$



Twelve Orifice Mixer
 $d/R = 0.34$



Fifteen Orifice Mixer
 $d/R = 0.30$



Eighteen Orifice Mixer
 $d/R = 0.28$

Figure 2. Schematic of Modules for $J=52$.

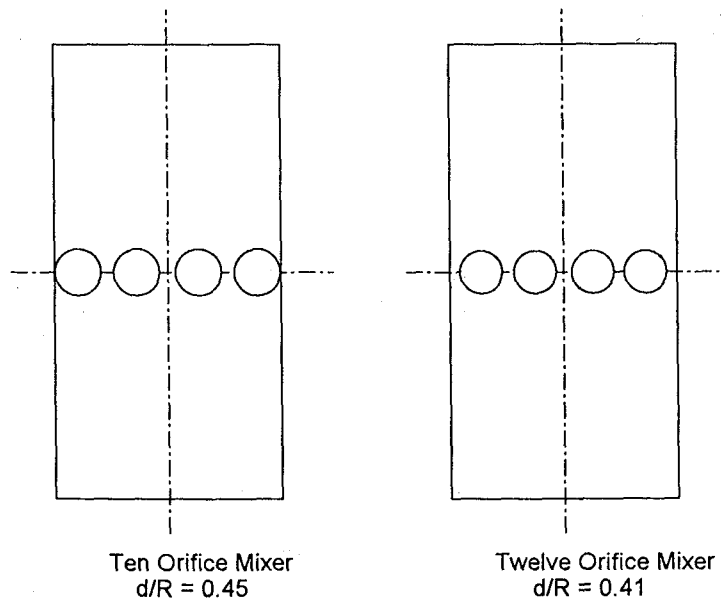
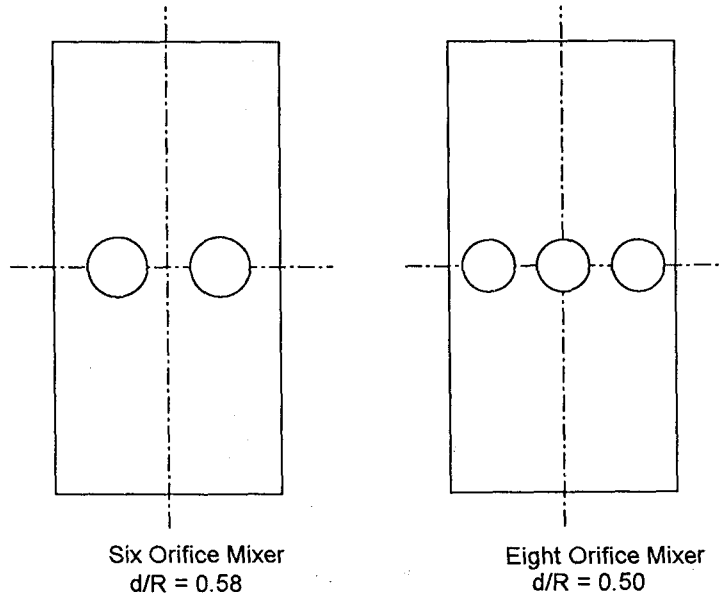


Figure 3. Schematic of Modules for $J=25$.

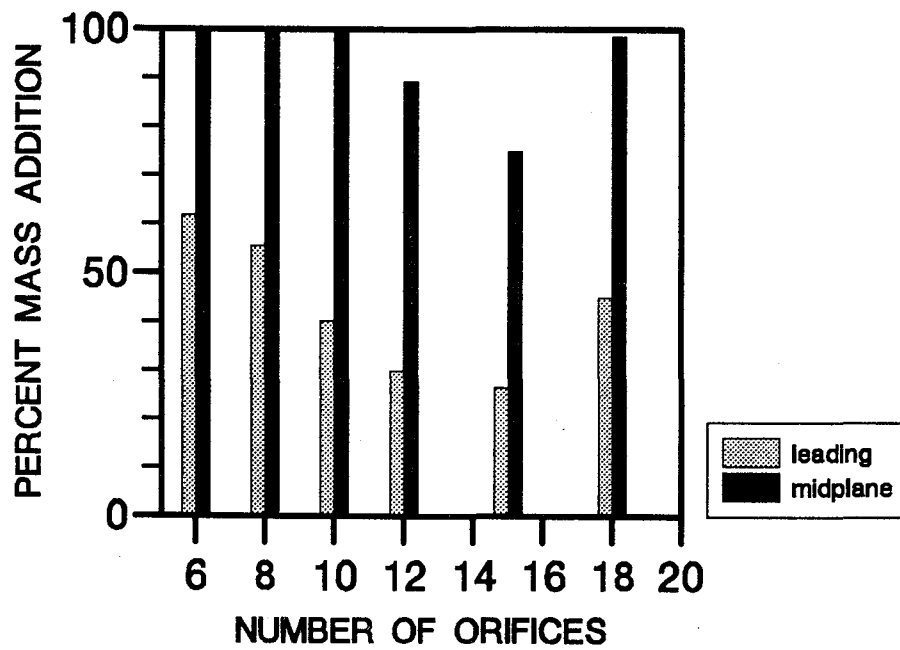


Figure 4. Jet Mass Added Per Plane for the J=52 Momentum Flux Ratio Modules as The Number of Orifices are Varied.

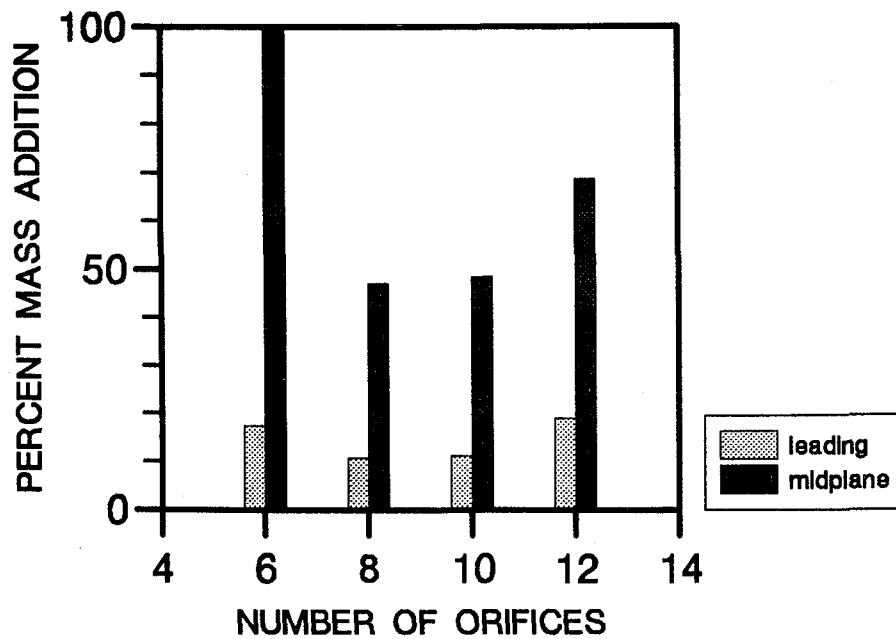


Figure 5. Jet Mass Added Per Plane for the J=25 Momentum Flux Ratio Modules as The Number of Orifices are Varied.

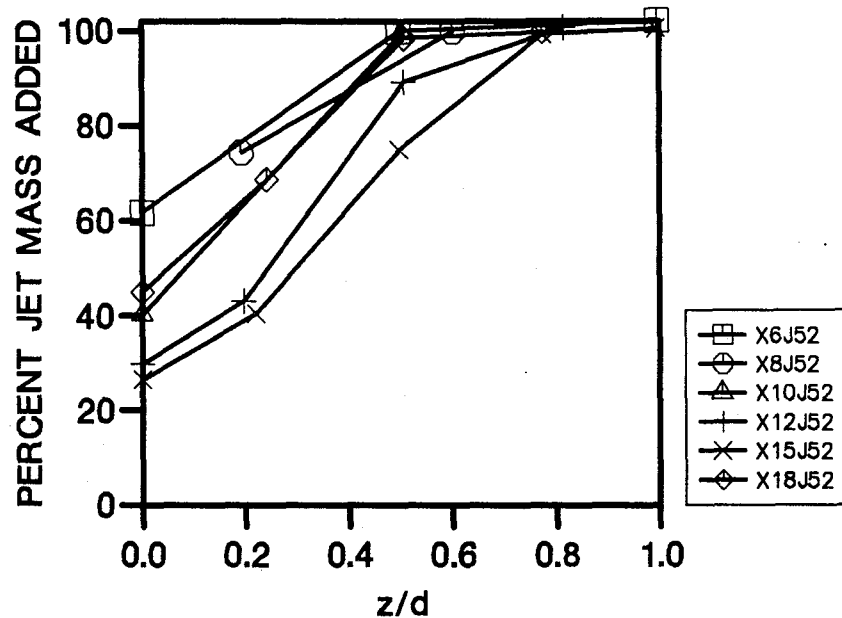


Figure 6. Jet Mass Added Per Plane for the J=52 Momentum Flux Ratio Modules Throughout the Orifice(Orifice Leading Edge=0, Orifice Trailing Edge=1).

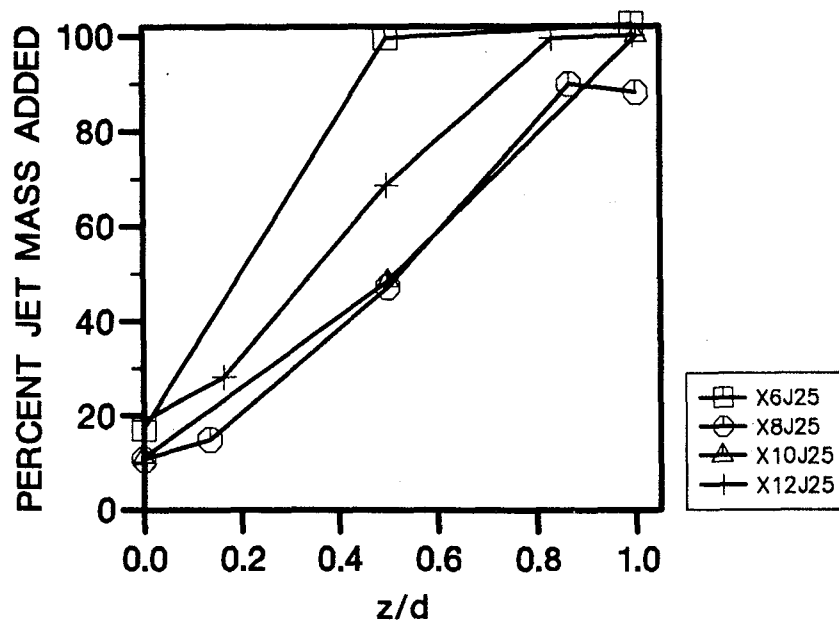


Figure 7. Jet Mass Added Per Plane for the J=25 Momentum Flux Ratio Modules Throughout the Orifice(Orifice Leading Edge=0, Orifice Trailing Edge=1).

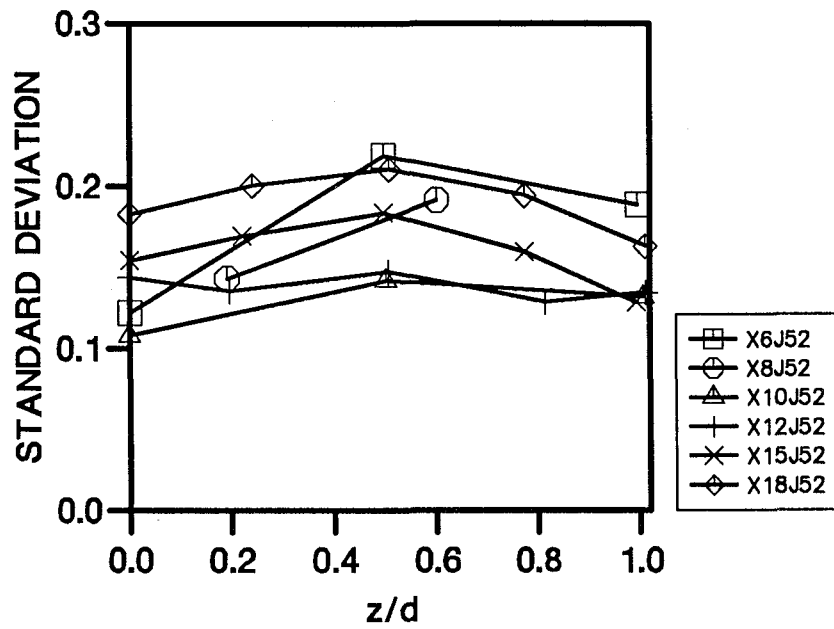


Figure 8. Area Weighted Standard Deviation Per Plane for the J=52 Momentum Flux Ratio Modules Throughout the Orifice (Orifice Leading Edge=0, Orifice Trailing Edge=1.)

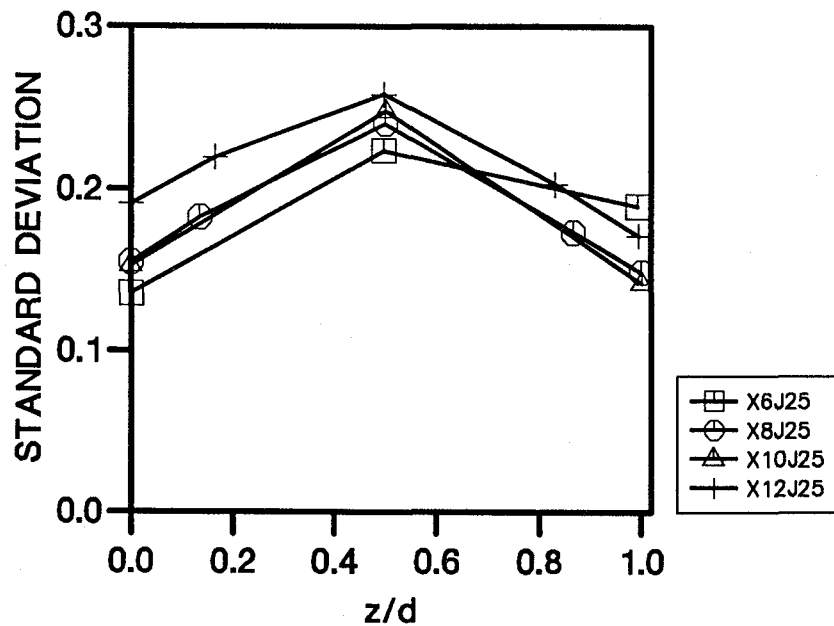


Figure 9. Area Weighted Standard Deviation Per Plane for the J=25 Momentum Flux Ratio Modules Throughout the Orifice (Orifice Leading Edge=0, Orifice Trailing Edge=1.)

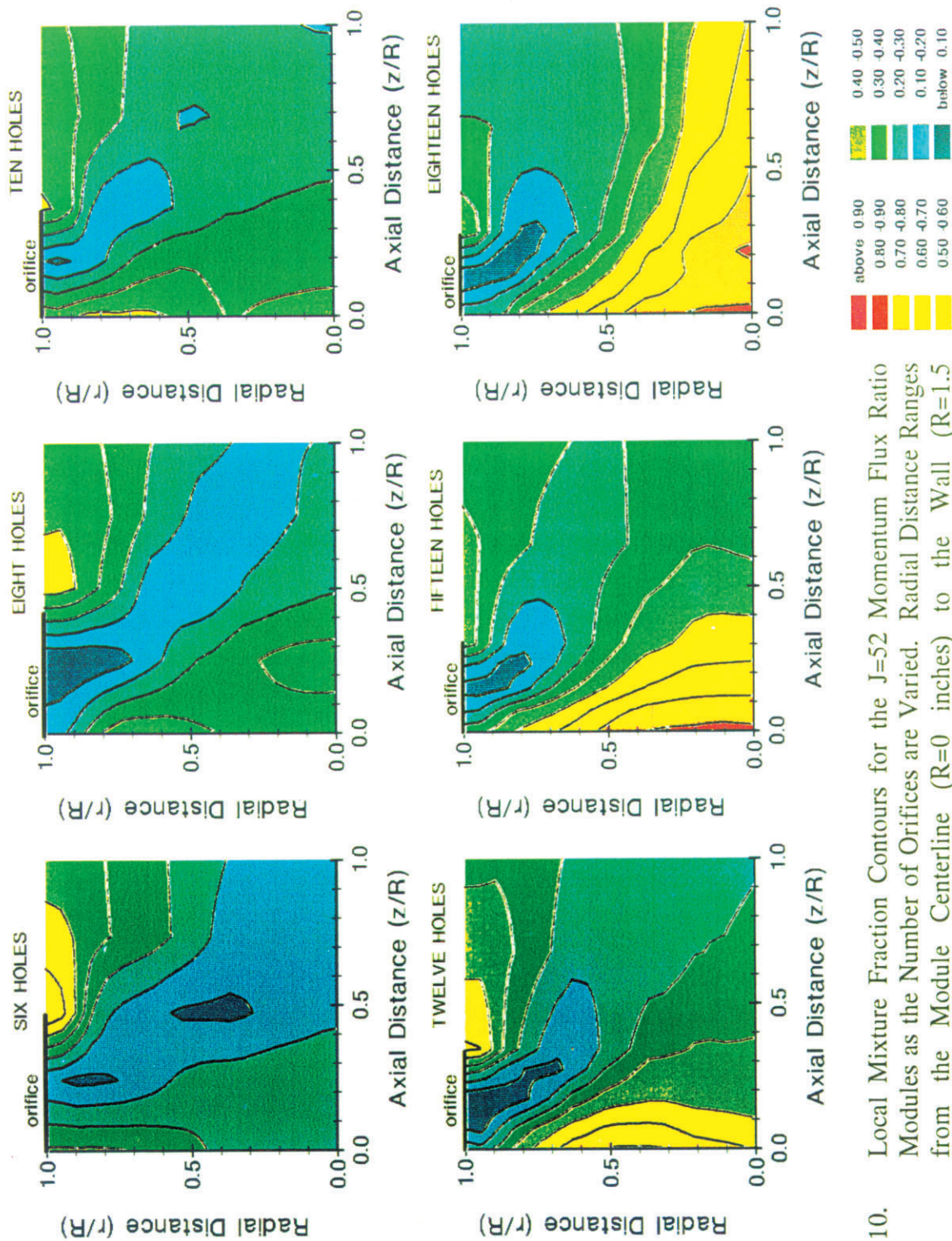


Figure 10. Local Mixture Fraction Contours for the $J=52$ Momentum Flux Ratio Modules as the Number of Orifices are Varied. Radial Distance Ranges from the Module Centerline ($R=0$ inches) to the Wall ($R=1.5$ inches). Axial Distance Ranges from the Orifice Leading Edge ($z=0$ inches) to One Duct Radius Downstream ($z=1.5$ inches).

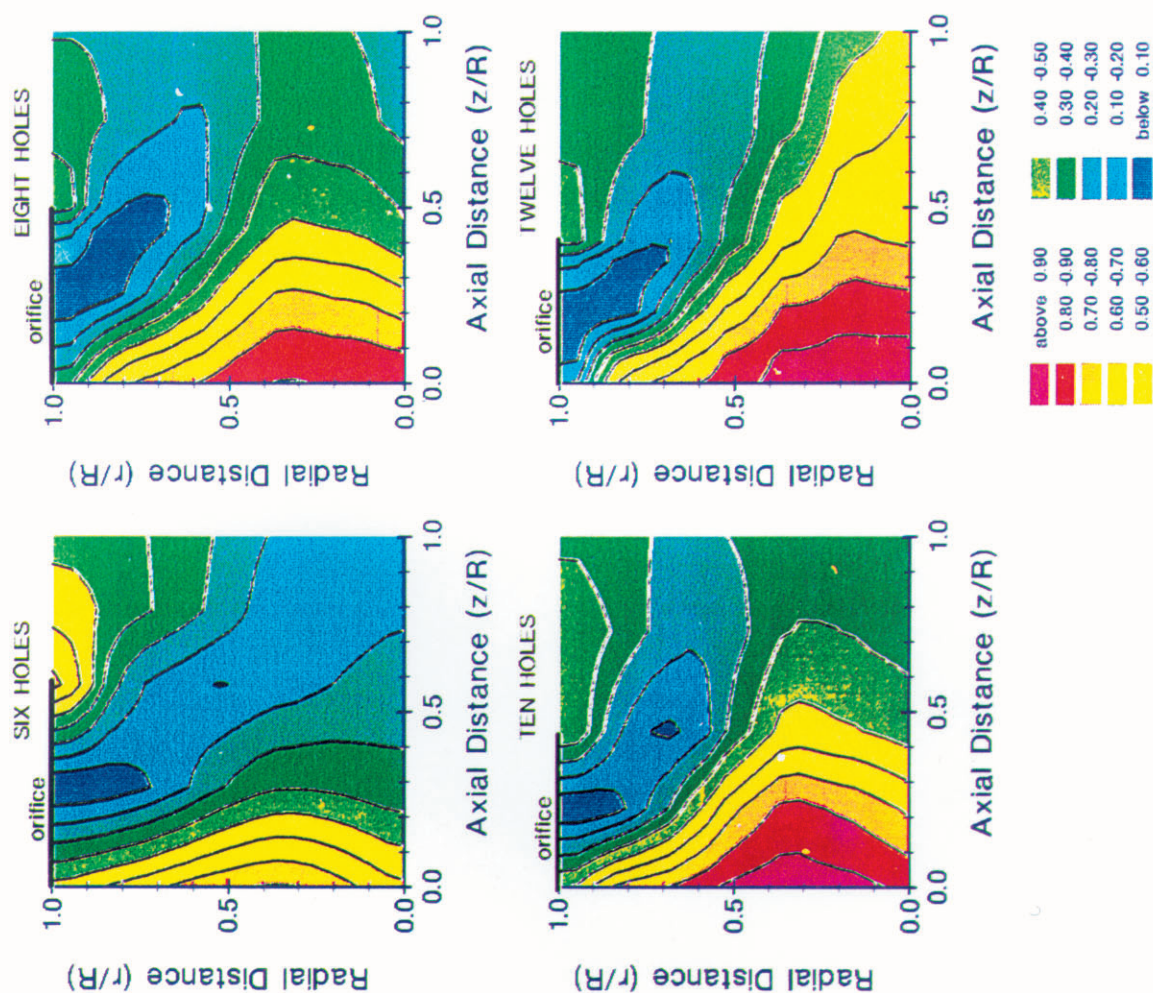


Figure 11. Local Mixture Fraction Contours for the $J=25$ Momentum Flux Ratio Modules as the Number of Orifices are Varied. Radial Distance Ranges from the Module Centerline ($R=0$ inches) to the Wall ($R=1.5$ inches). Axial Distance Ranges from the Orifice Leading Edge ($z=0$ inches) to One Duct Radius Downstream ($z=1.5$ inches).

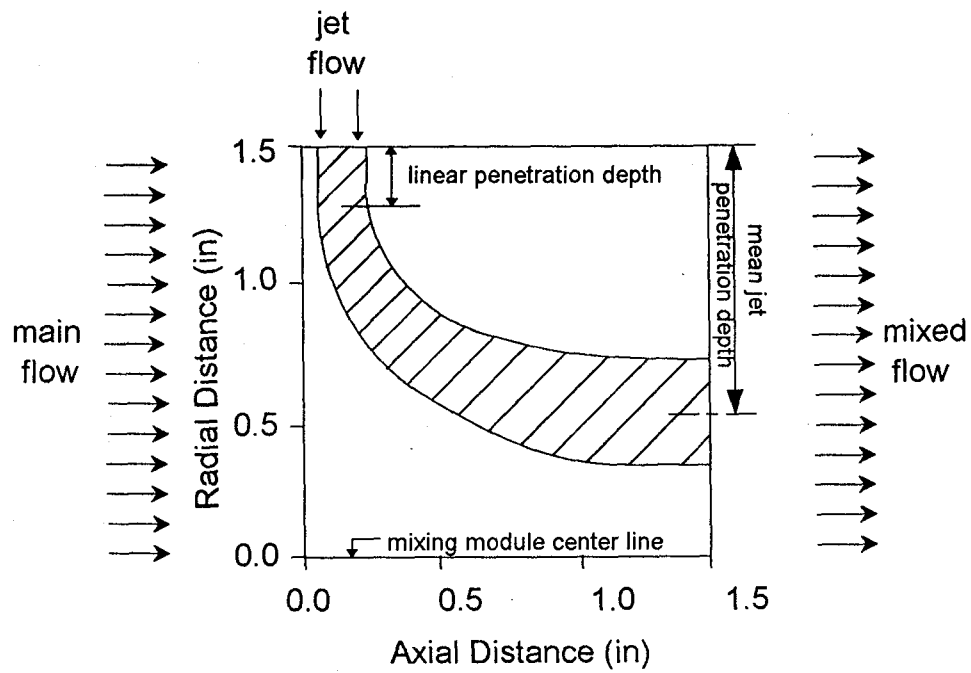


Figure 12. Example of Jet Trajectory Features Characterized.

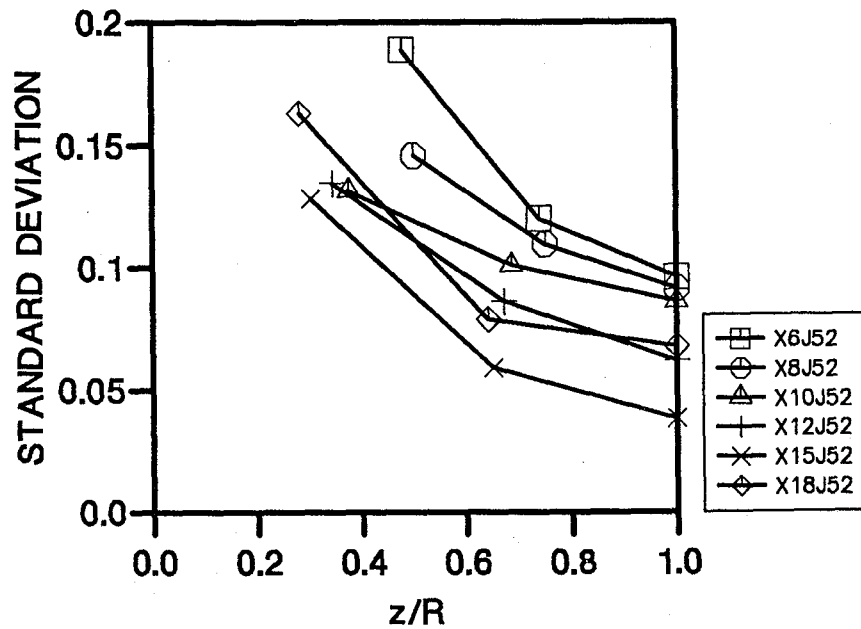


Figure 13. Area Weighted Standard Deviation Per Plane for the J=52 Momentum Flux Ratio Modules (Orifice Leading Edge=0, One Duct Radius Downstream=1.)

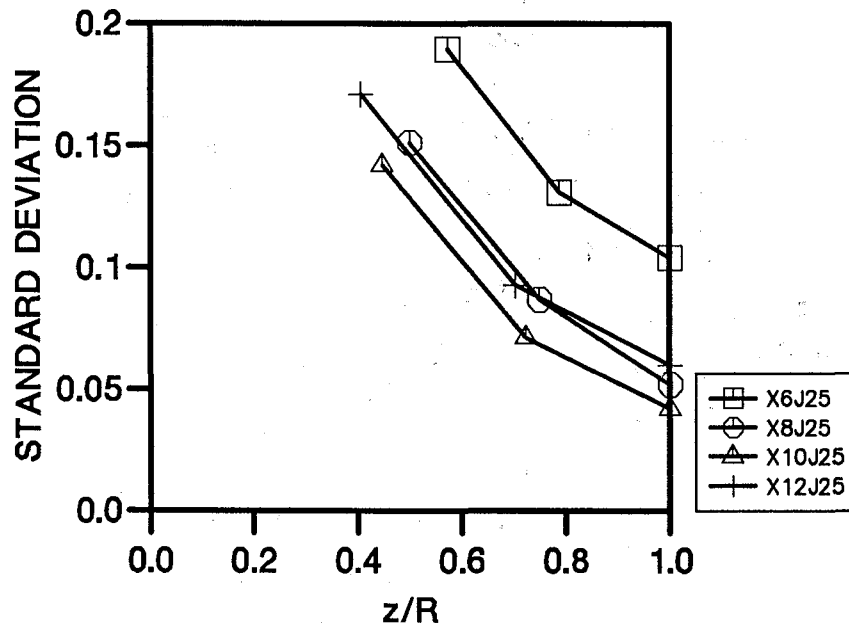


Figure 14. Area Weighted Standard Deviation Per Plane for the J=25 Momentum Flux Ratio Modules (Orifice Leading Edge=0, One Duct Radius Downstream=1.)

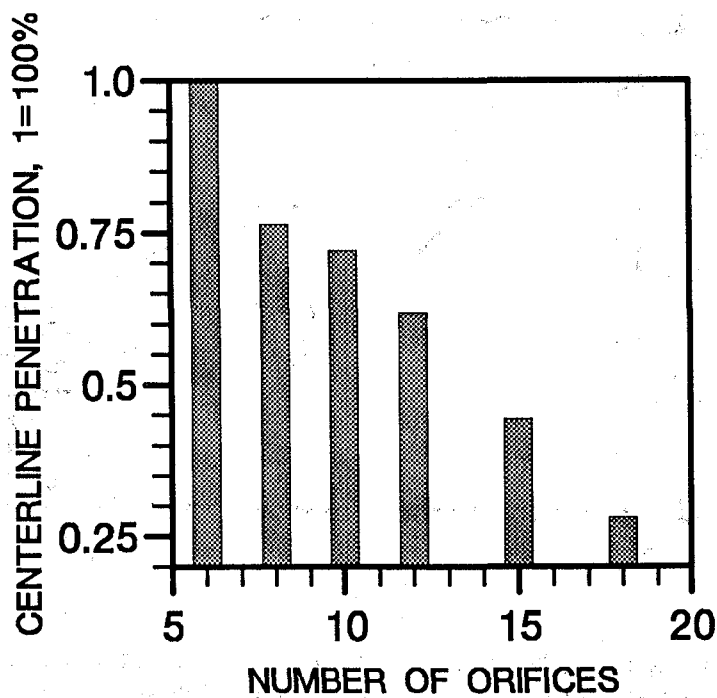


Figure 15. Mean Jet Trajectory Penetration Depth One Duct Radius Downstream of the Orifice Leading Edge for the J=52 Momentum Flux Ratio Modules.

REPORT DOCUMENTATION PAGE			Form Approved OMB No. 0704-0188	
Public reporting burden for this collection of information is estimated to average 1 hour per response, including the time for reviewing instructions, searching existing data sources, gathering and maintaining the data needed, and completing and reviewing the collection of information. Send comments regarding this burden estimate or any other aspect of this collection of information, including suggestions for reducing this burden, to Washington Headquarters Services, Directorate for Information Operations and Reports, 1215 Jefferson Davis Highway, Suite 1204, Arlington, VA 22202-4302, and to the Office of Management and Budget, Paperwork Reduction Project (0704-0188), Washington, DC 20503.				
1. AGENCY USE ONLY (Leave blank)		2. REPORT DATE January 1993		3. REPORT TYPE AND DATES COVERED Technical Memorandum
4. TITLE AND SUBTITLE Optimization of Circular Orifice Jets Mixing Into a Heated Cross Flow in a Cylindrical Duct			5. FUNDING NUMBERS WU-537-02-20-00	
6. AUTHOR(S) J.T. Kroll, W.A. Sowa, G.S. Samuelsen, and J.D. Holdeman				
7. PERFORMING ORGANIZATION NAME(S) AND ADDRESS(ES) National Aeronautics and Space Administration Lewis Research Center Cleveland, Ohio 44135-3191			8. PERFORMING ORGANIZATION REPORT NUMBER E-7508	
9. SPONSORING/MONITORING AGENCY NAME(S) AND ADDRESS(ES) National Aeronautics and Space Administration Washington, DC 20546-0001			10. SPONSORING/MONITORING AGENCY REPORT NUMBER NASA TM-105984 AIAA-93-0249 Corrected Copy	
11. SUPPLEMENTARY NOTES Prepared for the 31st Aerospace Sciences Meeting & Exhibit sponsored by the American Institute of Aeronautics and Astronautics, Reno, Nevada, January 11-14, 1993. J.T. Kroll, W.A. Sowa, and G.S. Samuelsen, University of California, UCI Combustion Laboratory, Irvine, California 92717-3550, and J.D. Holdeman, NASA Lewis Research Center, Cleveland, Ohio. Responsible person, J.D. Holdeman, (216) 433-5846.				
12a. DISTRIBUTION/AVAILABILITY STATEMENT Unclassified - Unlimited Subject Category: 07 Available electronically at http://gltrs.grc.nasa.gov/GLTRS This publication is available from the NASA Center for AeroSpace Information, (301) 621-0390.			12b. DISTRIBUTION CODE	
13. ABSTRACT (Maximum 200 words) To examine the mixing characteristics of circular jets in an axi-symmetric can geometry, temperature measurements were obtained downstream of a row of cold jets injected into a heated cross stream. The objective of the research was to obtain uniform mixing within one duct radius downstream of the leading edge of the jet orifices. An area weighted standard deviation of the mixture fraction was used to help quantify the degree of mixedness at a given plane. Non-reacting experiments were conducted to determine the influence of the number of jets on the mixedness in a cylindrical configuration. Results show that the number of orifices significantly impacts the mixing characteristics of jets injected from round hole orifices in a can geometry. Optimum mixing occurs when the mean jet trajectory aligns with the radius which divides the cross sectional area of the can into two equal parts at one mixer radius downstream of the leading edge of the orifice. The optimum number of holes at momentum-flux ratios of 25 and 52 is 10 and 15 respectively.				
14. SUBJECT TERMS Dilution; Jet mixing flow; Gas turbines; Combustion chamber; Can; Emissions			15. NUMBER OF PAGES 22	
			16. PRICE CODE A03	
17. SECURITY CLASSIFICATION OF REPORT Unclassified	18. SECURITY CLASSIFICATION OF THIS PAGE Unclassified	19. SECURITY CLASSIFICATION OF ABSTRACT Unclassified	20. LIMITATION OF ABSTRACT	